Unusual Hydrocarbon Chain Packing Mode and Modification of Crystallite Growth Habit in the Self-Assembled Nanocomposites Zinc−Aluminum-Hydroxide Oleate and Elaidate (*cis*- and *trans*- $[Zn_2Al(OH)_6(CH_3(CH_2)_7CH{=}CH(CH_2)_7COO^-)]$ and Magnesium Analogues

Zhi Ping Xu,[†,⊥] Paul S. Braterman,*[,†] Kui Yu,[‡,#] Huifang Xu,[§] Yifeng Wang,[∥] and C. Jeffrey Brinker[‡]

Departments of Chemistry and Materials Science, University of North Texas, P.O. Box 305070, Denton, Texas 76203, Advanced Materials Laboratories, Sandia National Laboratories, Albuquerque, New Mexico 87106, Department of Earth and Planetary Sciences, University of New Mexico, Albuquerque, New Mexico 87131, and Sandia National Laboratories, 4100 National Parks Highway, Carlsbad, New Mexico 88220

Received February 17, 2004. Revised Manuscript Received May 1, 2004

We report a novel packing mode specific to the cis unsaturated hydrocarbon chain in the title compound, a self-assembled layered double hydroxide−surfactant hybrid nanomaterial, and its influence on crystallite morphology and structure. The kink imposed by the cis double bond in oleate leads to partial overlap between chains on adjacent layers, with incomplete space filling, in contrast to the more usual (and more efficient) mono- and bilayer packings exhibited by the trans analogues. Incorporation of surfactant into the growing crystallite leads to a reversal of the usual LDH growth habit and results in crystallite shapes featuring ribbonlike sheets. The thermal decomposition behavior of the as-prepared organic/inorganic nanocomposites in air and N_2 is described.

Introduction

Layered double hydroxides (LDHs), also known as anionic (i.e., anion-exchanging) clays, are a family of naturally occurring or synthetic materials related to brucite, $Mg(OH)_2$, by isomorphous substitution of (usually) a divalent cation by a tervalent cation, leading to the incorporation of exchangeable anions and water molecules in the interlayer.[1,2] They have received intense attention in recent decades due to their wide applications as catalysts and catalyst precursors, anion absorbents, environment remediation and drug delivery agents, and components of polymer/clay composites. The introduction of long-chain organic anions into LDH leads to the formation of alternating metal hydroxide layer−organic anion layer hybrids, i.e., alternating inorganic/organic nanocomposite materials. It has been reported that many long-chain surfactant anions including alkyl carboxylates, alkyl sulfate, and alkyl sulfonates are intercalated by exchange, expanding the interlayer and rendering the surface hydrophobic.[3−7] In general, the hydrocarbon chains are closely packed either in a monolayer (strictly speaking, an interdigitated) mode, or in a bilayer mode, with the chains generally at a slanting angle with respect to the hydroxide layer. The interlayer spacing is strongly related to the chain length and packing mode, with self-assembly of the chains under the influence of hydrophobic forces.[3−7]

We report here a new packing mode specific to the cis unsaturated tail group (exemplified here by oleate, *cis*-$CH_3(CH_2)_7CH{=}CH(CH_2)_7COO^-$), for which the usual packing modes described above are not available, in contrast to the normal mono- and bi-layer packing modes of its otherwise similar trans analogue, *trans*-$CH_3(CH_2)_7CH{=}CH(CH_2)_7COO^-$, elaidate.

We also report that these hybrid organic−inorganic LDHs show novel particle morphologies and growth habits. In a conventional LDH, e.g., carbonate or chloride, the crystallites preferentially grow along the

* To whom correspondence should be addressed. E-mail: psb@unt.edu.
[†] University of North Texas.
[‡] Advanced Materials Laboratories, Sandia National Laboratories, Albuquerque, NM.
[§] University of New Mexico.
[∥] Sandia National Laboratories, Carlsbad, NM.
[⊥] Present address: Nanomaterials Centre (Nanomac), Division of Chemical Engineering, The University of Queensland, St Lucia, QLD 4072 Australia.
[#] Present address: Steacie Institute for Molecular Sciences, National Research Council Canada, Room 148A, 100 Sussex Drive, Ottawa, Ontario, Canada K1A 0R6.

(1) Cavani, F.; Trifiro F.; Vaccari, A. *Catal. Today* **1991**, *11*, 173.
(2) Rives, V.; Ulibarri, M. A. *Coord. Chem. Rev.* **1999**, *181*, 61.
(3) Kanoh, T.; Shichi, T.; Tagaki, K. *Chem. Lett.* **1999**, 117.
(4) Takagi, K.; Shichi, T.; Usami, H.; Sawaki, Y. *J. Am. Chem. Soc.* **1993**, *115*, 4339.
(5) Carlino, S. *Solid State Ionics* **1997**, *98*, 73.
(6) Meyn, M.; Beneke, K.; Lagaly, G. *Inorg. Chem.* **1990**, *29*, 5201.
(7) Braterman, P. S.; Xu, Z. P.; Yarberry, F. Chemistry of Layered Double Hydroxides. In *Handbook of Layered Materials*; Auerbach, S. M., Carrado, K. A., Dutta, P. K., Eds.; Marcel Dekker: New York, 2003.

10.1021/cm0497529 CCC: $27.50 © 2004 American Chemical Society
Published on Web 06/18/2004

Table 1. Observed XRD Data for Samples ZAO, MAO, ZAE, and ZAED

ZAO			MAO			ZAE			ZAED[b]			Miller indices
2θ/deg	d/nm[a]	(I/I0) (%)	2θ/deg	d/nm[a]	(I/I0) (%)	2θ/deg	d/nm[a]	(I/I0) (%)	2θ/deg	d/nm[a]	(I/I0) (%)	hkl
2.47	3.58	100	2.43	3.63	100	2.85	3.10	100	1.81	4.88	100	003
4.93	1.79	21.0	4.91	1.80	20	5.73	1.54	39.3	3.61	2.45	21.2	006
7.51	1.18	5.7	7.41	1.19	8.1	8.61	1.03	12.0	5.42	1.63	39.2	009
10.1	0.876	2.0	10.2	0.87	3.6	11.49	0.770	3.4	7.24	1.22	6.3	0,0,12
						14.45	0.613	2.0	9.08	0.974	12.5	0,0,15
						17.41	0.509	2.1	10.90	0.812	1.5	0,0,18
∼20	0.44	2.0	19.7	0.45	8.0	20.7	0.429	3.5	12.73	0.695	3.8	0,0,21
						23.2	0.384	2.0	14.59	0.607	1.0	0,0,24
						26.1	0.342	1.0	16.40	0.540	1.0	0,0,27
33.9	0.265	3.3	34.5	0.260	3.2	33.8	0.265	2.7	34.2	0.263	1.0	012
60.5	0.153	2.0	60.3	0.154	2.0	60.5	0.153	2.0	60.5	0.153	1.5	110
$a = 0.306$ nm, $c = 3 \times 3.56$ nm			$a = 0.308$ nm, $c = 3 \times 3.57$ nm			$a = 0.306$ nm, $c = 3 \times 3.08$ nm			$a = 0.306$ nm, $c = 3 \times 4.88$ nm			

[a] The average interlayer spacing was estimated as $(d_{003} + 2d_{006} + ... + nd_{00(3n)})/n$. [b] Only those data corresponding to the bilayer phase are listed.

a and *b* axes, giving hexagonal platelets with a lateral aspect ratio (*a*/*c*) of 10−30.[3,4,8] The materials described here, and LDH−anionic surfactant nanocomposites in general, adopt completely different morphologies, with preferred growth along the *c* axis, as shown by SEM and HRTEM, and we discuss this change in crystallite growth pattern in terms of molecular self-assembly and hydrophobic forces.[9]

Being interested in the possible production of our materials from low cost and naturally ocurring precursors, we selected a commercial olive oil (which contains oleate (70−80%), palmitate (∼11%), and linoleate (∼10%) triglycerides[10]) as the oleate source. We report that the one-pot preparation of oleate-like LDH, including in situ hydrolysis of olive oil in an alkaline solution, leads to formation of oleate-like LDH, as shown by XRD and FTIR.

The calcination of conventional LDHs leads generally to mixed metal oxides by way of dehydration, the collapse of hydroxide layers, and depletion of inorganic anions, and, in some cases, redox reactions of metal ions.[7,11] However, the decomposition of organic anions in surfactant LDHs is anticipated to be very different, as reported for MgCoAl−terephthalate LDHs.[12] In this paper, we describe the thermolysis of our materials under air and under N_2.

Most of this work was performed using Zn:Al LDH, as it is our experience that these show better crystallinity than their Mg:Al analogues, as well as higher contrast in TEM for the metal hydroxide layers. The few experiments we did perform with Mg:Al LDH confirm the expectation that the two systems would behave similarly.

Experimental Section

1. Preparation of Materials. The precursor layered double hydroxide $Zn_2Al(OH)_6Cl{\cdot}nH_2O$ was prepared, then thoroughly washed via centrifuge and dried in a vacuum over molecular sieves, as described elsewhere.[13,14] Briefly, 50 mmol $AlCl_3{\cdot}6H_2O$ (Aldrich, 99%) and 150 mmol $ZnCl_2{\cdot}6H_2O$ (Aldrich, 98%) were dissolved in 500 mL of pure water (18.2 MΩ cm). After being purged with N_2 for around 30 min, the solution was treated with 15.7 mL of 50% NaOH (300 mmol, Alfa Aesar), followed by an overnight reflux under a slow stream of N_2. Thus the metal stoichiometry is controlled by the amount of added base while excess Zn^{2+} is present in solution. The precipitate was collected and thoroughly washed with deionized water via centrifuge, and dried in a vacuum over molecular sieves. This precursor was used to prepare organic LDH by the exchange method. Samples ZAO (Zn_2Al-LDH−oleate) and ZAE (Zn_2Al-LDH−elaidate) were obtained by exposing the precursor (ca. 4 mmol) to 100 mL of a colloidal solution containing oleate (ca. 6 mmol) or elaidate (ca. 4 mmol), and refluxing overnight. The surfactant solutions were prepared by dispersing potassium oleate paste (40% w/w in water, Aldrich) in water or elaidic acid (6.0 mmol, 98%, Avocado) in aqueous NaOH (6.0 mmol). After separation and thorough washing, the samples were dried in a vacuum over molecular sieves. In comparison, ZAED (Zn_2Al-LDH−*excess* elaidate) was prepared in a similar way but using 150% excess elaidate, i.e., 10 mmol exchanging with 4 mmol precursor LDH. We also carried out several preparations of Zn_2Al-LDH−elaidate with 5−100% excess elaidate present. The filtrate in all cases has a pH of 10−11. Mg_2Al-LDH compounds with these two anions were prepared similarly.

The one-pot method (i.e., precipitating metal ions in anion-containing basic solution and refluxing overnight) gave LDH compounds of similar composition. In some experiments, a commercial olive oil was used as the oleate precursor for a one-pot preparation of Mg_2Al-LDH−oleate. In a typical preparation, 2.413 g of $AlCl_3{\cdot}6H_2O$ (10 mmol, Aldrich, 99%) and 4.067 g of $MgCl_2{\cdot}6H_2O$ (20.0 mmol, Aldrich, 99%) were dissolved in 150 mL of deionized water, and then mixed with 3.62 g of olive oil (MW = 860−900, 4.0−4.2 mmol, i.e., 12.0−12.6 × 80% = ∼10.0 mmol oleate) and treated with 3.7 mL of 50% NaOH solution (71 mmol, Alfa Aesar). This mixture was heated to reflux overnight and followed by a separation, washing, and drying procedure similar to that for ZAO and ZAE, giving an Mg:Al LDH product (sample name MAO).

2. Materials Characterization. Powder diffraction patterns were collected on a powder X-ray diffractometer (XRD, Siemens F-series) with Cu Kα ($\lambda = 0.15418$ nm) radiation at a scanning rate of 1.2° per minute from $2\theta = 2°$ to $2\theta = 65°$. Powdered CaF_2 was used as an internal calibrant, and the *d* spacing was calculated from the several orders of basal reflections as described in Table 1. Infrared spectra were collected using KBr disks on a Perkin-Elmer 1760X FTIR after 40 scans within 4000−400 cm^{-1} at a resolution of 4 cm^{-1}. SEM images were taken on a JEOL T 300 microscope at a voltage of 20 kV and a filament current of around 5 mA. TEM was

(8) Cai, H.; Hillier, A. C.; Franklin, K. R.; Nunn, C. C.; Ward, M. D. *Science* **1994**, *266*, 1552.
(9) Xu, Z. P.; Braterman, P. S. *J. Mater. Chem.* **2003**, *13*, 268.
(10) Kuksis, A. *Fatty acids and Glycerides*; Plenum Press: New York, 1978; pp 225 and 359.
(11) Xu, Z. P.; Zeng, H. C. *J. Mater. Chem.* **1998**, *8*, 2499.
(12) Xu, Z. P.; Zeng, H. C. *J. Phys. Chem. B* **2000**, *104*, 10206.
(13) Boclair, J. W.; Braterman, P. S. *Chem. Mater.* **1999**, *11*, 298.
(14) Boclair, J. W.; Braterman, P. S.; Jiang, J. P.; Lou, S. W.; Yarberry, F. *Chem. Mater.* **1999**, *11*, 303.

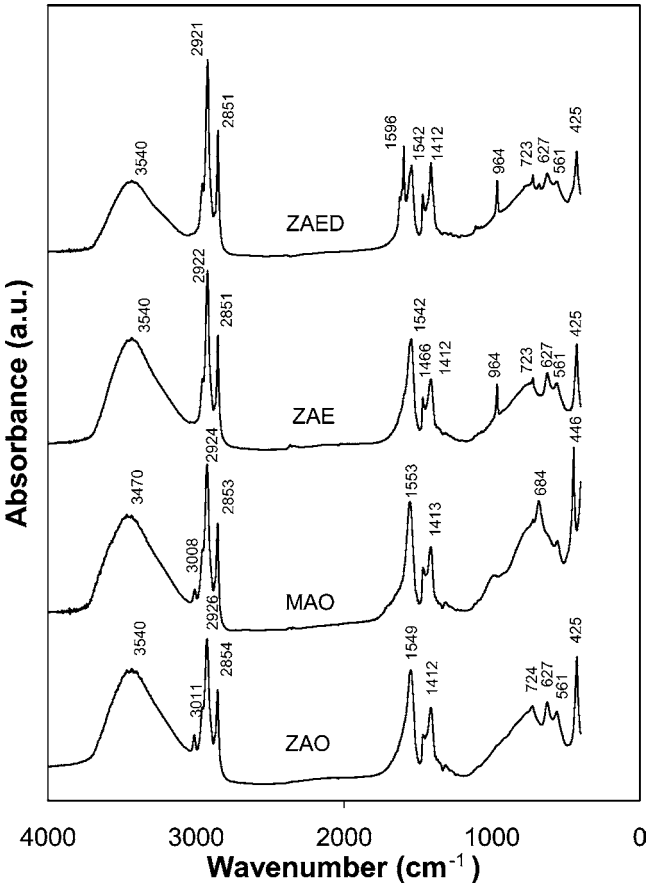

Figure 1. FTIR spectra of samples ZAO, ZAE, ZAED, and MAO.

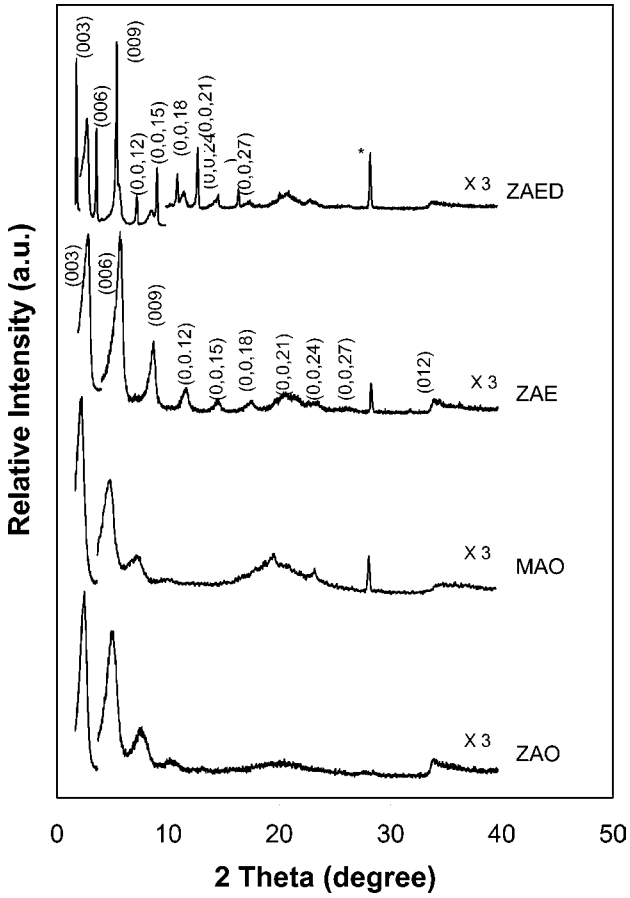

Figure 2. XRD patterns of samples ZAO, ZAE, ZAED, and MAO. The peak marked with an asterisk (*) is from internal calibrant CaF_2. The peak between (003) and (006) for ZAED is attributed to ZAE impurity.

performed on a JEOL JEM-100 CXII electron microscope at a voltage of 100 kV and a filament current of 80−85 μA.

Zinc, magnesium, and aluminum content was determined by atomic absorption (AAnalyst 300, Perkin-Elmer). Carbon and hydrogen contents were measured with CHN analyzer by MHW laboratories. Found for ZAO, 41.2% C, 6.66% H, 24.2% Zn, and 5.23% Al, with atomic ratios C/Zn/Al = 17.7:1.91:1; and for ZAE, 40.3% C, 7.20% H, 22.2% Zn, and 5.05% Al with atomic ratio C/Zn/Al = 18.0:1.81:1. Calculated for both $Zn_2Al(OH)_6(oleate)\cdot H_2O$ and $Zn_2Al(OH)_6(elaidate)\cdot H_2O$, 38.7% C, 7.33% H, 22.8% Zn, and 4.84% Al with ratios 18:2:1. Found for MAO, 45.6% C, 8.48% H, 10.5% Mg, and 5.45% Al with atomic ratio C/Mg/Al = 18.8:2.14:1. Calculated for both $Mg_2Al(OH)_6(oleate)\cdot H_2O$ 45.2% C, 8.58% H, 10.3% Mg, and 5.65% Al, assuming all anions are oleate.

The presence of free acid in ZAED was confirmed and determined by a back-titration method. In general, 0.2−0.4 mmol LDH was dissolved in excess HCl solution (5.00 mmol) with gentle heating, then the excess H^+ and elaidic acid were titrated with an NaOH solution (0.100 N) by monitoring the pH to the end point of 6−7, using NaF (2−4 mmol) and $HOCH_2CH_2OH$ (4−8 mmol) as the masking agents of Al^{3+} and Zn^{2+},[15] respectively. The results showed that the molar ratio of free elaidic acid to Al was 0.50:1. The elemental analyses found for ZAED, 46.8% C, 7.92% H, 18.4% Zn, and 3.95% Al with atomic ratio C/Zn/Al = 26.6:1.92:1; calcd for both $Zn_2Al(OH)_6(elaidate)(elaidic\ acid)_{0.5}\cdot 0.5H_2O$, 46.9% C, 8.25% H, 18.9% Zn, and 3.90% Al, with ratio 27:2:1.

Thermogravimetric analysis (TGA, Perkin-Elmer, TGA6) was carried out in both oxidizing (air) and inert (N_2) atmospheres. During the measurement, 10−15 mg of sample was heated at a rate of 10 °C/min with a gas flow rate of 100 mL/min over a temperature range of 30−800 °C.

(15) Dean, J. A. *Analytical Chemistry Handbook*; McGraw-Hill: New York, 1995; pp 2.12−2.13.

Results and Discussion

1. Structural Features. As shown in Figure 1, ZAO, ZAE, and MAO show the common IR characteristics of long-chain carboxylate LDH compounds. These include a broad band at ~3500 cm^{-1} (ν_{OH} of layer hydroxide),[1,2] a group of strong peaks at 2800−3000 cm^{-1} (asymmetric and symmetric ν_{CH}),[16,17] two strong bands at 1400−1600 cm^{-1} (asymmetric and symmetric $\nu_{C=O}$) and δ_{CH2} at 1466 cm^{-1}, as well as bands at 724 (δ_{CH}),[16−18] 627, 561, and 425 cm^{-1} (ν_{MO}).[1,2] However, there are also more distinctive features: ν_{CH} attached to a double bond in ZAO (3011 cm^{-1})[17] and MAO (3008 cm^{-1}),[17] and δ_{CH} (out-of-plane deformation) for elaidate in sample ZAE at 964 cm^{-1}.[17] It is worth mentioning that the sharp peak at 446 cm^{-1} in sample MAO indicates the formation of a well-ordered 2:1 Mg:Al LDH.[19,20] The characteristic peaks of asymmetric and symmetric ν_{CH} at 2800−3000 cm^{-1} are actually identical in MAO and ZAO, confirming the intercalation of the oleate hydrocarbon chain. In addition, we note an extra peak at 1596 cm^{-1} for sample ZAED only. This extra peak is attributed to the asym-

(16) Williams, D. H.; Fleming I. *Spectroscopic Methods in Organic Chemistry*, 4th ed.; McGraw-Hill: New York, 1989.

(17) Simons, W. W., Ed. *The Sadtler Handbook of Infrared Spectra*; Sadtler Research Laboratories, Inc.: Philadelphia, PA, 1978; pp 26, 710, and 741.

(18) Borja, M.; Dutta, P. K. *J. Phys. Chem.* **1992**, *96*, 5434.

(19) Xu, Z. P.; Zeng, H. C. *J. Phys. Chem. B* **2001**, *105*, 1743.

(20) Kloprogge, J. T.; Frost, R. L. *J. Solid State Chem.* **1999**, *146*, 506.

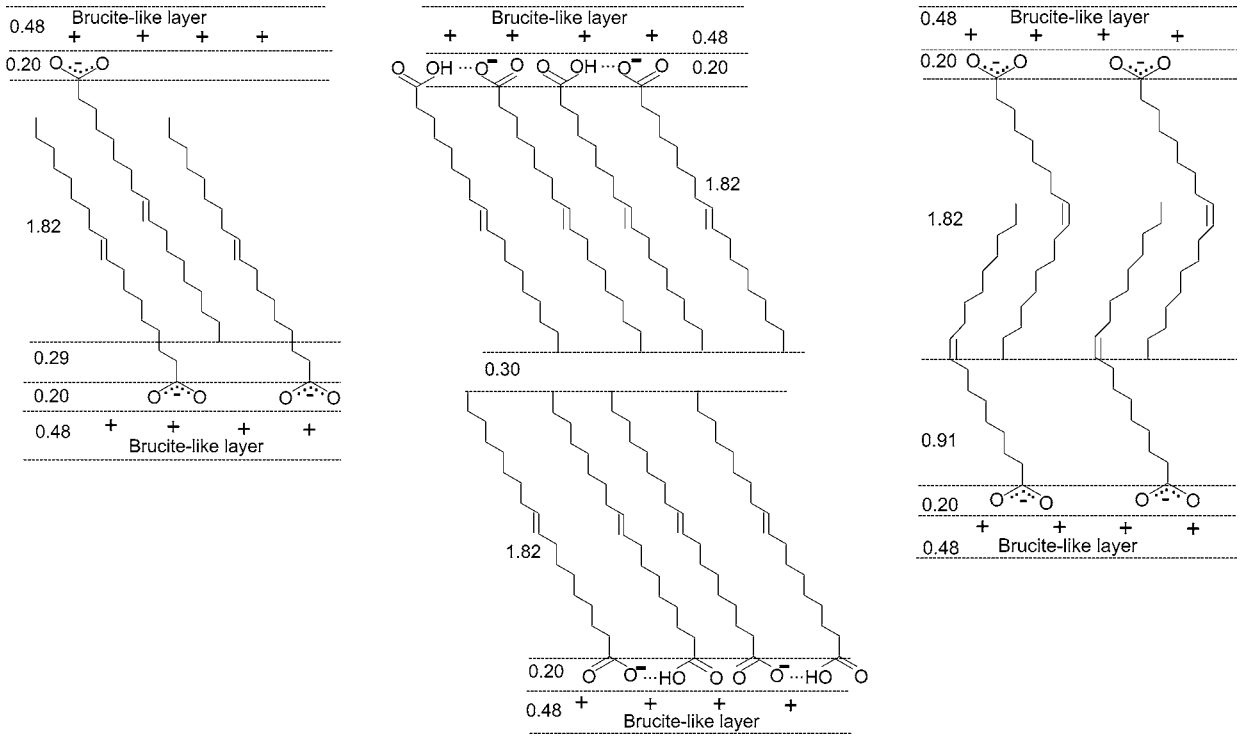

Figure 3. Proposed packing of (a) elaidate, (b) elaidate/elaidic acid, and (c) oleate in the interlayer; distances in nm.

metric $\nu_{C=O}$ of an undissociated carboxylic acid group (COOH) that is H-bonded in the interlayer in sample ZAED,[18] as also required by the back-titration data and elemental analyses reported above. The intercalation of such free acid groups[20] is a general phenomenon, when excess carboxylate anions are used in the exchange or preparation, even at such high pH.[21]

Powder X-ray diffraction patterns in Figure 2 show strong basal reflections (*00l*),[1,2] as expected for an expanded layer structure. The 2θ angles, corresponding *d* spacings, and relative intensities are summarized in Table 1. It is calculated from the reflections that the interlayer spacing is 3.56 nm for ZAO and 3.57 nm for MAO, the identity of which further confirms that they have the same intercalated anion: oleate. There is a consistent reflection series for sample ZAE, up to the ninth reflection order, i.e., (*0,0,27*) peak, indicating an average spacing of 3.08 nm. However, the XRD patterns of sample ZAED comprise not only the series of reflections of ZAE, but also a new series of much sharper reflection peaks, as indicated by bold indexes in Figure 2. These new reflections correspond to an interlayer spacing of 4.88 nm. We have found in other experiments in this series that 5−10% excess elaidate can lead to the formation of this new phase. Therefore, ZAED contains two discrete LDH phases, in which the intercalated species (elaidate/elaidic acid) are presumed to pack in monolayer and bilayer modes, as addressed in the following section.

The nominal particle thickness in the *c*-axis direction was calculated from the measured widths of peaks *(00l)*, using the Debye−Scherrer equation without instrument correction,[22] to be 20−30 nm for samples ZAO, MAO, and ZAE, and 70−80 nm for the new phase in ZAED. We also note that peak (*0,0,21*) of ZAE overlaps a broad reflection, presumably associated with the hydrocarbon chains in the interlayer;[9] such a broad band is also observed for all other samples in the same region.

2. Anion Packings. If the chains of these two anions were completely extended and tilted at about 55°, as is usual for straight chain carboxylate LDH,[5,6,23] their vertical height in LDH would be the same (1.82 nm for the hydrocarbon chain, refer to Figure 3a and b). Thus, such an antiparallel packing mode implies an overall basal spacing of 2.99 nm for an extended C_{18} chain anion.[3,4] This is in good agreement with the spacing found for elaidate (3.08 nm, sample ZAE) and for saturated carboxylates.[24] Additionally, the implied tilting of the hydrocarbon chains in the interlayer at ca. 55° is similar to the tilting habit in saturated fatty acids in their crystals (∼60°),[25] and allows both carboxylate oxygen atoms to form hydrogen bonds to the hydroxide layers equally.

If excess elaidate/elaidic acid is used in the exchange, then a new phase (4.88 nm, in sample ZAED) is also formed, corresponding to a bilayer packing as plotted in Figure 3b. The interlayer spacing is predicted to be 4.82 nm, in quantitative agreement with that observed in sample ZAED. We note that elaidic acid is intercalated as such even at pH up to 11 and we attribute this to H-bonding of the free acid with carboxylate and/or pendant layer hydroxide groups.[24] It is known that the asymmetric $\nu_{C=O}$ of free elaidic acid is 1715 cm^{-1}.[17] The

(21) Xu, Z. P.; Braterman, P. S.; Seifollah, N. Abstract in *Proceedings of the 224th ACS National Meeting*, Boston, MA, Aug. 18−22, 2002; p Coll. 219.

(22) Cullity, B. D. *Elements of X-ray Diffraction*, 2nd ed.; Addison-Wesley: Boston, MA, 1978; p 278.

(23) Lagaly, G. *Angew. Chem., Int. Ed. Engl.* **1976**, *15*, 575.

(24) Gunstone, F. D. *An Introduction of the Chemistry and Biochemistry of Fatty Acid and Their Glycerides*, 2nd ed.; Chapman and Hall Ltd.: London, 1967; pp 70−74.

(25) Xu, Z. P.; Braterman, P. S. Layered Double Hydroxides: Multiple Phases and Self-Assembly. In *Encyclopedia of Nanoscience and Nanotechnology*; Marcel Dekker: New York, 2003.

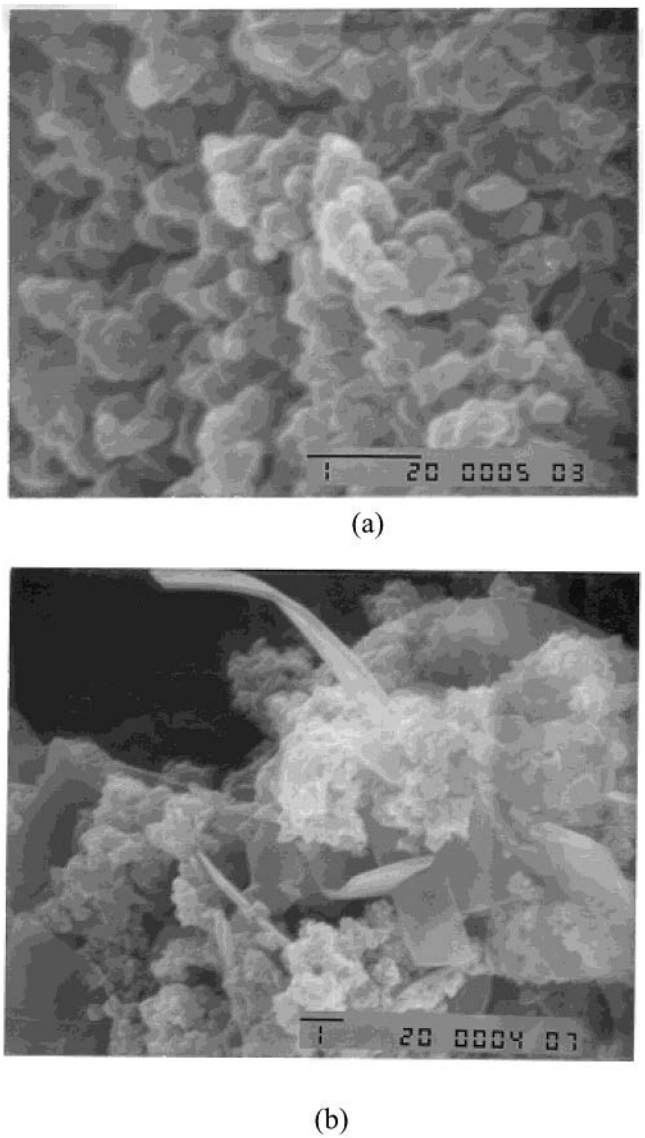

Figure 4. Scanning electron micrographs of (a) ZAO and (b) ZAE; scale bar 1 μm.

shift to 1596 cm^{-1} further supports the formation of an H-bond involving the free acid group (COOH) in the interlayer.[18] Similar infrared features have also been observed for LDHs with intercalated stearate/stearic acid.[3,24]

However, oleate requires a packing mode different from the above two cases (Figure 3c) because the cis geometry imposes a bend in the middle of the chain which prevents the full overlapping described above. In fact, this bend allows the chains to overlap only in the region below the double bond (Figure 3c), sticking the chains together like Velcro. The calculated spacing (3.61 nm) for this packing mode is quite close to that observed (3.56 or 3.57 nm). The bending geometry of oleate in the LDH interlayer is similar to the boomerang shape that oleic acid employs in its crystallization.[25] Though 50% excess oleate was used in the exchange, no new phase like that in ZAED is observed. The situation for MgAl-LDH−oleate is similar.

3. Morphology and Growth Habit. The different packing in the interlayer gives rise to different morphologies, as shown in Figure 4. There are homogeneous submicron platy sheets in ZAO (Figure 4a), whereas

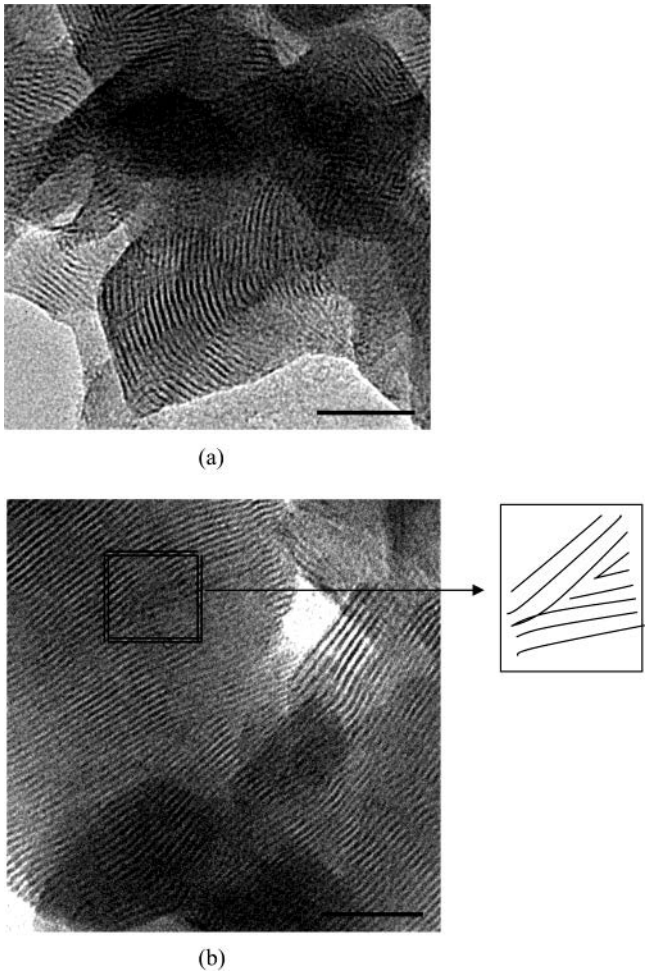

Figure 5. Transmission electron micrographs of (a) ZAO and (b) ZAE; scale bar 50 nm.

ZAE gives much bigger sheets or ribbons with length and width in micrometers, as shown in Figure 4b,[26] although small irregular particles are scattered around. These features are clearly quite different from the regular hexagonal platy sheets of inorganic LDH.[3,4,8,26,27]

As further shown in Figure 5, TEM images directly display the stacking of hydroxide or organic anion layers. The strongly scattering (metal hydroxide layer) and weakly scattering (anion layer) stripes are alternating and roughly parallel. We note that sample ZAE has larger uniform stacking regions than sample ZAO and that the average fringe distances are 3.3 nm for ZAE and 3.5 nm for ZAO, in tolerable agreement with the XRD observation. We also note the layer bending and layer merging or branching as indicated in the insert of the figure.

We suggest that these features are related to a major difference between the growth habit of hybrid organo-LDH crystallites and that of inorganic LDH. It is known that crystallites of inorgano-LDHs grow along the *a* and *b* axes to form hexagonal thin sheets, which tend to lie flat with the *c* axis perpendicular to the plane of the support. Thus, it is in general difficult to directly observe the stacking of hydroxide layers in TEM. However, we have clearly observed the layer stacking in ZAO and

(26) Ogawa, M.; Asai, S. *Chem. Mater.* **2000**, *12*, 3253.
(27) Labajos, F. M.; Rives, V.; Ulibarri, M. A. *J. Mater. Sci.* **1992**, *27*, 1546.

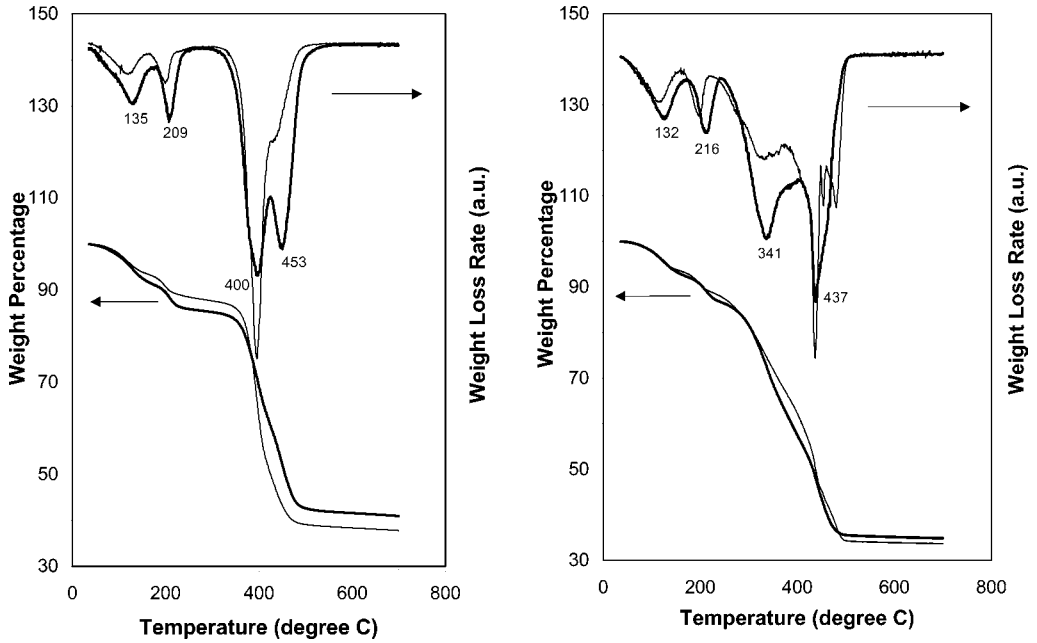

Figure 6. TGA and differential TGA curves of samples ZAO and ZAE in N_2 (a) and air (b). The bold curves belong to sample ZAO whose differential TGA peaks are marked.

ZAE. The ribbonlike sheets observed in SEM for ZAE and the corresponding alternation of black and white stripes clearly show that the crystallites have grown along the *c* axis.

We attribute this to self-assembly of surfactant-rich layers by hydrophobic interactions at the *ab* plane of the growing crystallite. The positively charged hydroxide layers bind the hydrophilic heads of the anions on the plane via electrostatic interactions, leaving their tails to form a thin, self-assembled, hydrophobic layer. This hydrophobic layer adsorbs another layer of anions with antiparallel orientation, which provides a nucleus for the next layer, thus promoting growth along the *c* axis.

4. Thermal Decomposition. The thermal decomposition processes of samples ZAO and ZAE in air and N_2 are shown in the TGA and differential TGA curves of Figure 6. As summarized in Table 2, there are four main stages of thermolysis. The first two stages are not influenced by the atmosphere in which the thermolysis takes place.[1,2,7] The first event is unambiguously attributed to loss of absorbed water molecules, in which the observed weight loss of 7.9−8.9% for ZAO and 7.2% for ZAE is in good agreement with the calculated 8.0% for ZAO and 7.1% for ZAE from the loss of 2.4 and 2.2 water molecules per formula unit, respectively. (There are more waters than found by elemental analysis, due to less rigorous predrying.) We tentatively assign the second step to partial dehydroxylation of the layer structure. In this stage, the weight loss is 5.1−5.4% for ZAO and 4.2−4.8% for ZAE, about half of the 9.2% and 8.8% respectively estimated for total dehydroxylation.

The major event in the third stage, involving decomposition of organic species as well as further dehydroxylation, is more complicated. In the N_2 environment (Figure 6a), ZAE shows one sharp weight loss while ZAO shows two weight losses around 400 °C. Decomposition in air, however, begins at as low as 250−300 °C, and is followed by a second process at around 450 °C (Figure 6b). Presumably decomposition of the organic species takes place by several parallel and/or serial processes, as previously reported,[12] such as dehydrogenation, thermal cracking to various hydrocarbons, decarboxylation and/or oxidation to CO_2, and graphitization.

In an inert environment more hydrocarbons are generated through thermal cracking and less CO_2 is formed. By contrast, dehydrogenation and oxidation are major processes in air due to the sufficient oxygen supply, taking place at low temperatures. However, it is not so clear why there is a second process appearing at around 450 °C under air. We would suggest that the early oxidation, like burning, occurs mainly on the particle surface and forms a compact oxide film. This oxide film may hinder the diffusion of oxygen and delay the oxidation of inner organic species. Such behavior may prove useful in flame retardance.

Table 2. Weight Losses (%) and Thermal Events of Samples ZAO and ZAE in Air and N_2

	in air	in N_2	calcd.[a]	thermal events
			temp 40−175 °C	
ZAO	7.9	8.9	8.0	dehydration
ZAE	7.2	7.2	7.1	
			temp 175−240 °C	
ZAO	13.3	14.0	17.2[b]	partial dehydroxylation
ZAE	12.0	11.4	15.9[b]	
			temp 240−600 °C	
ZAO	64.9	58.5		further dehydroxylation and decomposition of organic anions
ZAE	66.1	61.7		
			temp 600−800 °C	
ZAO	65.4	63.3	63.8[c]	decomposition of carbonate salts and some carbon residues
ZAE	66.6	66.6	65.2[c]	

[a] The calculation of weight loss percentage is based on nominal formula: $Zn_{1.91}Al(OH)_{5.82}(oleate)_{0.98}\cdot 2.4H_2O$ for ZAO and $Zn_{1.81}Al(OH)_{5.62}(Elaidate)_{1.00}\cdot 2.2H_2O$ for ZAE. [b] The weight loss calculated accounts for full dehydration and dehydroxylation. [c] The final oxide has a nominal formula $Zn_{1.91}AlO_{3.41}$ for ZAO and $Zn_{1.81}AlO_{3.31}$ for ZAE.

We suggest, on the basis of the weight loss and an earlier report, [28] that stage four consists of carbonate decomposition and, in air, burning of carbon residues. The final weight losses at 800 °C in both cases are in quantitative agreement with the calculation from nominal chemical formulas (Table 2) assuming metal oxides are the only products.

Conclusions

In conclusion, when two cis−trans isomers (oleate and elaidate anions) are intercalated into Zn_2Al- and Mg_2-Al-LDH interlayer, they show different packing modes and morphologies. Like saturated straight chain organic anions, elaidate packs either in an antiparallel (monolayer) or bilayer mode based on the amount used. The bilayer mode involves intercalation of the free carboxylic acid, even at high pH. For oleate, however, its boomerang shape imposes hook-like partial overlap, which prevents the chains from packing in the above modes but allows a Velcro-like partial overlap. This arrangement implies a less efficient use of space, and the existence of a pattern of molecular scale pores.

For both anions, the growth habit is completely different from that generally found for inorganic LDH, being dominated by *c*-axis preferred growth (in the elongated LDH described by Miyata and Okada,[29] the morphology was inherited from a needlelike magnesium hydroxide precursor). There are, however, detailed differences between our two cases. Bigger, platy, ribbonlike sheets (flat, bent, or twisted) are typical of LDH elaidate, whereas smaller, irregularly shaped, platy sheets are found in LDH oleate. In addition, the complete overlapping of hydrocarbon chains in LDH elaidate results in much better crystallinity than that in LDH oleate, as shown by the more extended orderly regions evident in the TEM images, and the clearer XRD pattern, of ZAE compared with ZAO.

Thermolysis of these and other organic/inorganic hybrids reveals four major decomposition steps either in air or nitrogen, withthe third step, i.e., the decomposition of organic species, being different in the two atmospheres.

Acknowledgment. We thank the Robert A. Welch Foundation (Grant B-1445), Sandia National Laboratories' Laboratory Directed Research and Development Program (LDRD award 26554), and the University of North Texas Faculty Research Fund, for support, and Dr. Susanta K. Saha for assistance with the Figures. Sandia is a multiprogram laboratory operated by Sandia Corporation, a Lockheed Martin company, for the United States Department of Energy's National Security Administration under Contract DE-AC04-94AL85000.

CM0497529

(28) Tsuji, M.; Mao, G.; Yoshida, Y.; Tamaura, Y. *J. Mater. Res.* **1993**, *8*, 1137.

(29) Miyata, S.; Okada, A. U.S. Patent 4351841, 1982.